Development of the High Voltage Hall Accelerator System

IEPC-2019-901

Presented at the 36th International Electric Propulsion Conference
University of Vienna • Vienna, Austria
September 15-20, 2019

Hani Kamhawi[1], Luis Pinero[2], Jonathan Mackey[3], Wensheng Huang[4], John Yim[5], Dragos Dinca[6], and Carol Tolbert[7]
National Aeronautics and Space Administration, Glenn Research Center, Cleveland, Ohio, 44135

and

Vlad Shilo[8]
Colorado Power Electronics, Inc., Fort Collins, Colorado, 80542

Abstract: NASA Glenn Research Center (GRC) is pursuing the development of a 4.5-kilowatts (kW) Hall thruster propulsion system. The main components of the system include the High Voltage Hall Accelerator (HiVHAc) Hall thruster, a wide input and output range power processing unit (PPU) developed by Colorado Power Electronics (CPE), and a xenon flow control unit developed by VACCO Industries. This paper provides an update on the status of the system development. The HiVHAc thruster design has been updated to enable operation at discharge power levels of 4.5 kW. The updated thruster design, designated HiVHAc+, incorporates a centrally mounted cathode and an optimized magnetic field topology. Preliminary performance evaluation of HiVHAc+ measured thrust efficiencies of 58% at 4.5 kW. CPE is continuing the development of a 4.5-kW-class prototype development unit (PDU). The PDU design incorporates complete form, fit and function for flight and all electrical, electronic and electromechanical parts that are rad-hard, space-qualified parts or have exact equivalents. The PDU is scheduled for delivery to NASA GRC in the Spring of 2020. NASA's Announcement of Collaborative Opportunities program is funding qualification and system integration test campaigns of the PDU PPU with NASA and commercial Hall thrusters.

I. Introduction

Electric propulsion (EP) systems can enable and enhance NASA's ability to perform scientific space exploration. NASA's Science Mission Directorate (SMD) performs planetary science missions to small bodies including fly-by, rendezvous, and sample return from a diverse set of targets [1]. NASA missions have successfully employed EP systems on the Deep Space 1 and Dawn missions [2, 3]. To augment its capability to perform these and other solar system exploration missions, NASA continues to develop advanced EP technologies. Small body mission studies indicate that the majority of these small body missions are enabled by the use of EP, and nearly all of the small body missions of interest are enhanced with EP [4].

[1] Senior Research Engineer, Electric Propulsion Systems Branch, Hani.Kamhawi-1@nasa.gov.
[2] Senior Research Engineer, Electric Propulsion Systems Branch, Luis.r.Pinero@nasa.gov.
[3] Research Engineer, Electric Propulsion Systems Branch, Jonathan.a.Mackey@nasa.gov.
[4] Senior Research Engineer, Electric Propulsion Systems Branch, Wensheng.Huang@nasa.gov.
[5] Senior Research Engineer, Electric Propulsion Systems Branch, John.t.Yim@nasa.gov.
[6] Lead Electrical Engineer, Electrical Power System Branch, Dragos.Dinca@nasa.gov.
[7] Project Manager, Space Science Project Office, Carol.m.Tolbert@nasa.gov.
[8] Senior Engineer, Colorado Power Electronics Inc, vshilo@c-pwr.com.

Electric propulsion system performance can significantly reduce launch vehicle requirements, costs, and spacecraft mass because of its high specific impulse capability when compared to chemical propulsion. One study found that significant cost savings can be realized by use of EP when compared to chemical propulsion for NASA Discovery class missions [5].

Earlier mission studies [5] evaluated the performance of the High Voltage Hall Accelerator (HiVHAc) 3.5-kilowatts (kW) class thruster propulsion system for four NASA Discovery class design reference missions (DRMs) that included:

- Vesta-Ceres rendezvous mission (i.e., Dawn Mission), which has both time constraints and a very high post launch ΔV, requiring both a moderate thrust-to-power and a higher specific impulse than a conventional Hall thruster;
- Koppf comet rendezvous mission, which has few constraints and does not require thruster operation in gravity wells (this favors a high specific impulse throttle table);
- Near-Earth Asteroid Return Earth Return (NEARER) mission; and
- Nereus sample return (NSR) mission, which is a relatively low ΔV mission with time constraints favorable for a higher thrust-to-power thruster.

Results from the mission studies indicated that the HiVHAc propulsion system was able to exceed the needs of all the evaluated missions but improved mission performance can be achieved if the system can operate at both high thrust-to-power and high specific impulse (not simultaneously).

Attaining high specific impulse and high thrust-to-power operation required a power processing unit (PPU) that supply discharge voltages up to 600-V and discharge currents up to 15 A, while not exceeding a total discharge power of 4.5-kW. Additionally, NASA's science missions required a PPU that can operate at variable input voltage range to accommodate the spacecraft power management system's supplied voltage. To that end, NASA GRC is working with Colorado Power Electronics (CPE) to mature the design of a 4.5 kW PPU with an input voltage range of 68-V to 140-V and an output voltage range of 200-V to 700-V for implementation in NASA's HiVHAc propulsion system [6, 7]. As for the HiVHAc thruster, NASA GRC improved the thruster design so it can operate at discharge power levels of 4.5-kW. The new thruster was designated HiVHAc+ and additional details about the thruster are presented in upcoming sections.

This paper presents an update on NASA GRC's continued development of the HiVHAc Hall propulsion system. The paper is arranged as follows: Section II presents an overview of the HiVHAc Hall thruster propulsion system and presents a summary of the development status of the three major HiVHAc subsystems; Section III details the experimental test setup implemented in this current test campaign; Section IV presents a summary of the HiVHAc+ thruster tests results; Section V presents a summary of the HiVHAc system upcoming development activities and plans; and Section VI presents a summary of the paper.

II. Hall Propulsion System Overview

The major elements of the dual-mode long-life Hall propulsion system that is being developed and matured by NASA Glenn Research Center (GRC) are shown in Figure 1 and they include:

- The HiVHAc+ thruster. The HiVHAc+ thruster development was funded by NASA's Space Technology Mission Directorate (STMD) Center Innovation Fund (CIF). Under CIF funding, NASA GRC designed, manufactured, and performed preliminary thruster characterization tests;
- The CPE PPU. The HiVHAc project is utilizing a PPU that is being designed and developed by CPE. NASA's Small Business Innovative Research (SBIR) Commercialization Readiness Program (CRP) project is funding further maturation of the CPE PPU to TRL6; and
- The VACCO xenon flow control module (XFCM) was designed and developed by VACCO Industries [8, 9]. It was extensively tested under the HiVHAc project. The unit is being leveraged by the Advanced Electric Propulsion System (AEPS) project and is the baseline xenon flow control (XFC) module for AEPS.

Additional details on the development the various HiVHAc+ subsystems are provided in upcoming sections.

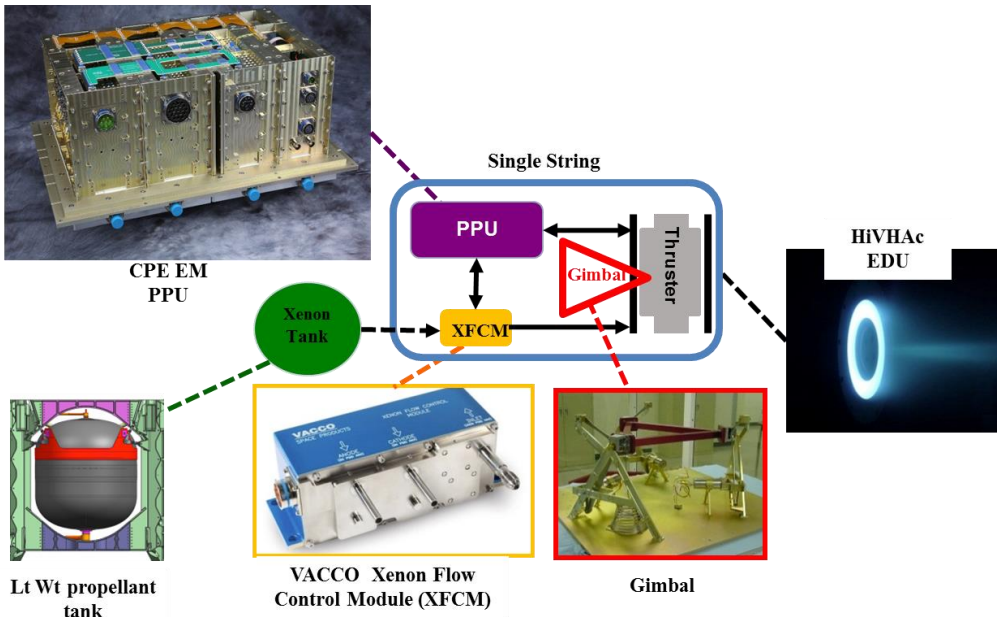

Figure 1. HiVHAc propulsion system layout showing the HiVHAc engineering development unit, CPE EM PPU, and VACCO XFCM.

HIgh Voltage Hall Accelerator + (HiVHAc+)

The HiVHAc+ thruster is a higher power version of the HiVHAc thruster [5, 10, 11]. The HiVHAc+ thruster design, manufacturing, and tests were funded by NASA's STMD CIF program. The HiVHAc+ thruster design incorporates the many lessons learned from the HiVHAc thruster development and is also designed to provide performance attributes that meet the commercial geosynchronous orbit (GEO) market orbit-raising and station-keeping propulsion needs with a robust thruster design that results in operation that is invariant with facility pressure. The 4.5 kW HiVHAc+ thruster incorporates several features that enable higher performance and higher propellant throughput than SOA Hall thrusters, including:

1) It implements a NASA-patented magnetic circuit design that extends its propellant throughput capability when compared to state-of-the-art (SOA);
2) It incorporates a centrally mounted cathode. The centrally mounted cathode has been found to improve thruster performance, reduce plume divergence, and improve coupling between the cathode and the thruster's discharge, thus reducing ground facility effects [12]; and
3) It implements a NASA-GRC-patented propellant manifold assembly [13] that is also being implemented on the Advanced Electric Propulsion System (AEPS) 12.5-kW flight thrusters by Aerojet Rocktdyne (AR); and

The thruster was designed at NASA GRC using magnetic modeling, thermal modeling, and flow modeling tools. The thruster mechanical design was then completed and its manufacturing was performed at NASA GRC. The thruster hollow cathode assembly was purchased from Plasma Controls, LLC. The cathode assembly was custom designed for integration with the HiVHAc+ thruster. The Plasma Controls cathode assembly is a heaterless cathode assembly. The insert material is based on a novel low work function insert that was developed by Colorado State University.[14] Figure 2 shows a photograph of the HiVHAc+ thruster with heaterless cathode assembly installed. A brazed hollow cathode assembly based on the NASA GRC heritage design is being manufactured and will be integrated with the HiVHAc+ thruster for upcoming component and system level tests.

A. Colorado Power Electronics Prototype Development Unit Power Processing Unit

Development of a HiVHAc PPU is being performed by CPE. The CPE PPU development started in 2008 with a Phase I SBIR contract. CPE was then awarded a Phase II to develop a brassboard PPU. After the successful completion of the Phase II effort additional SBIR contract awards were made that culminated in an engineering model (EM) PPU unit that was extensively tested by NASA GRC [7].

The EM PPU has form, fit and most functionality for flight. A block diagram of the EM PPU is shown in Figure 2. It consists of two discharge modules that operate in parallel to supply up to 4.0 kW of power to the thruster through an innovative 3-phase resonant converter topology capable of providing full output power at any output voltage between 200-V and 700-V. It also has an auxiliary module that includes two electromagnet, cathode keeper and cathode heater power supplies. Lastly, housekeeping power supplies, XFCM drivers and a digital control interface unit (DCIU) are included in the DCIU module. The DCIU provides autonomous control of the PPU power supplies and the XFCM. Algorithms to conduct system control sequences for cathode conditioning, cathode ignition, discharge start-up, steady-state discharge current regulation, throttling and shutdown are completely parametrized to enable tailoring to different thrusters. The DCIU also processes telemetry from the PPU and XFCM and transmits it to the spacecraft computer over a MIL-STD-1553 interface. A photograph of the EM PPU is shown in Figure 3.

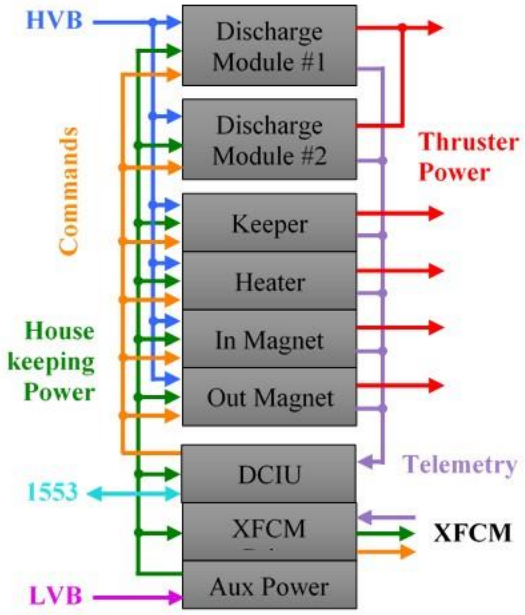

Figure 2. Block diagram of the EM PPU.

The EM PPU was subjected to extensive testing at GRC that included performance and functional verification tests in air and vacuum environments [7]. While in vacuum, performance and functionality was also verified at temperatures ranging from -20˚C to 50˚C. Efficiencies as high as 95% were measured at a power level of 4.0-kW. An electromagnetic interference (EMI) test was done to characterize conducted emissions (CE01 and CE03 requirements) per MIL-STD-461C on both high voltage (80-V to 160-V) and low voltage inputs (24-V to 34-V) into the PPU. Integrated system level testing of the EM PPU was also successfully performed with both the HiVHAc and SPT-140 thrusters [15]. During these integration tests, thruster performance was measured and discharge oscillations were characterized. Discharge initiation in hard, soft and glow mode was successfully demonstrated as well as the ability to throttle, regulate discharge current, and operate different Hall thrusters.

Figure 3. Photograph of the EM PPU.

Work towards a prototype development unit (PDU) started in 2016. CPE was awarded a Phase III NASA SBIR Commercialization Readiness Program (CRP) project to further the maturation of the EM PPU. Under the CRP project, NASA's Science Mission Directorate, NASA GRC, and JPL in partnership with NASA's SBIR program co-funded the development of the PDU PPU. The PDU includes complete form, fit and function for flight and utilizes all electrical, electronic and electromechanical parts that are rad-hard, space-qualified or have exact equivalents. The PDU includes some design changes to further enhance capabilities and meet interface requirements. It has higher discharge power capability up to 4.5-kW. The PDU also has a modified input voltage range of 68-V to 140-V to better satisfy commercial spacecraft bus voltages and still satisfy typical NASA deep space missions power requirements. Output requirements for the thruster electromagnet and heater power supplies were also extended to capture the requirements of multiple thrusters including NASA's HiVHAc+ and Hall effect rocket with Magnetic Shielding (HERMeS) as well as commercial Hall thrusters. Additional features of the PDU include electromagnet polarity reversal and discharge current ripple telemetry.

The preliminary design review for the PDU was completed in November 2016 and a critical design review including action items were completed in February 2018. Parts stress, thermal, structural, reliability and worst-case analyses have been completed. The PDU fabrication is on-going using applicable flight processes and quality standards. The PPU is expected to be delivered to NASA GRC in the spring of 2020. Table 1 below summarizes key electrical characteristics.

Table 1: CPE PDU PPU Key Electrical Characteristics.

PDU PPU	Discharge	Magnets (2)	Keeper	Heater
Output Voltage	200 – 700 V	2 – 20 V	5 – 40 V	1 – 13 V
Output Current	1.4 – 15 A	1 – 7.5 A	1 – 2 A	3.5 – 21 A
Output Power Max	4.5 kW	108 W	80 W	210 W
Regulation Mode	Voltage or Current	Current	Current	Current
Output Ripple	≤ 5%			
Line/Load Regulation	≤ 2%			
Input Voltage	68 – 140 V (main) and 24 – 34V (housekeeping)			

B. VACCO Xenon Flow Control Module

The VACCO XFCM is the baseline xenon feed system for the HiVHAc propulsion system [8]. The XFCM development was funded by NASA and the Air Force Research Laboratory. The XFCM is a highly integrated feed system that provides independent flow control to the anode and cathode, and provides pressure and flow rate monitoring on each propellant flow outlet. A block diagram of the XFCM is shown in Figure 4a. The unit utilizes two redundant micro-latching valves, two piezoelectric control valves, passive flow restrictors, and input and output pressure and temperature transducers to enable flow metering. After qualification tests of the XFCM unit, it was extensively tested with the HiVHAc, SPT-140, and HERMeS TDU-1 thruster. [15] The AEPS XFC is a derivative of the XFCM. The AEPS XFC flow schematic and mechanical packaging is shown in 4b and is almost identical to the XFCM.

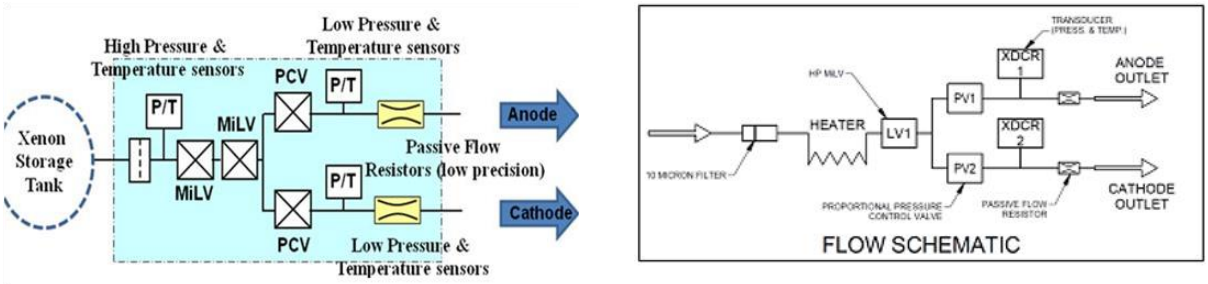

(a) **(b)**

Figure 4. Schematics of the VACCO XFCM and XFC units.

III. HiVHAc+ Test Setup

Testing of the HiVHAc+ thruster was performed in vacuum facilities VF-3 and VF-6 at NASA GRC.[16] Flow uniformity tests of the HiVHAc+ were performed in VF-3 and hot fire performance characterization tests were performed in VF-6. The VF-3 main chamber is 1.5-m in diameter and is 4.5-m long, it is evacuated with 4 oil diffusion pumps. The VF-6 main chamber is 7.6-m in diameter, 18.3-m long, and is evacuated with 12 internal nude cryo pumps.

A. VF-3 Flow Uniformity Test Setup

During the flow uniformity test, the fully assembled HiVHAc+ thruster was mounted on top of a rotary stage to control the azimuthal coordinate of the interrogation point. The pressure probe was mounted on top of two cross-mounted stages. One stage was responsible for controlling the axial coordinate while the other controlled the radial coordinate. The azimuthal stage could position the test article with an accuracy of 0.5° and a precision of 0.01°. The axial and radial stages had accuracies of 0.1 mm and precisions of 2 µm.

Research-grade xenon was supplied to the test article using a commercially available mass flow controller with a flow rate uncertainty of ±1% of reading. Background pressure was monitored via two nude ion gauges located 0.6 m from the thruster. The averaged background pressure varied from $4x10^{-4}$ to $7x10^{-4}$-Torr-Xe over the range of the tested mass flow rates. The uncertainty of the facility pressure was estimated by the manufacturer to be within ±6% of reading.

To measure the pressure in the test article, a micro-ion gauge with extended pressure measurement range was deployed. This gauge was a hot filament gauge capable of measuring pressure from $5x10^{-10}$ to $5x10^{-2}$-Torr on air. The accuracy of this sensor as stated in the manufacturer's specification is 10%. However, precision is expected to be better than 10% if used over a short period of time. To ensure the precision of the data was good, data at one azimuthal plane was obtained at the beginning and the end of each mass flow rate condition. The precision of the sensor was found to be on the order of 1%. A 90-degree elbow pitot-style tube was deployed to reduce the interrogation point to a region about 4 mm in diameter. The interrogating tip of the tube was sharpened to a 45° angle in order to deflect gas particles that are outside of the interrogation point.

The test was conducted via a dedicated data acquisition computer, which was running a custom Labview program. The computer communicated with the motion controllers, which commanded the motion stages. The computer also communicated with a commercial data acquisition device, which measured the analog output of the pressure sensor controller. During the test, the computer automatically orchestrated the sequence of events including stage motion, appropriate wait time and data recording. Probe settling time, defined as the time the probe system takes to read 95% of the total change in pressure after a sharp change in pressure was characterized to be 2.5-sec to 3.0-sec. The computer was set to wait 5-sec before taking data after the probe was moved into each new measurement location.

B. VF-6 Power Supplies, Data Acquisition, and Control Systems

For the HiVHAc+ test campaign the thruster was powered with a laboratory power rack that contained the discharge, inner and outer electromagnet, cathode heater, and cathode keeper power supplies. The data acquisition system used for the HiVHAc+ tests was a multiplexed datalogger with computer interface. The datalogger monitored the voltages, currents, temperatures, propellant flow rates, chamber pressure, and thrust at 1 Hz during performance testing. The computer interface had the additional benefit of allowing a number of channels to be monitored with failsafe limits for unattended operation. The uncertainties of the data logger measurements were ±0.05% for the voltage and current measurements [17].

C. VF-6 Flow System

A laboratory propellant feed system was used in the HiVHAc+ test campaign. The feed system supplied xenon to the thruster. The propellant feed system utilized four mass flow controllers (MFC). A 500-sccm and 50-sccm MFCs supplied xenon propellant to the thruster and cathode, respectively. The MFCs calibration curves indicated that the anode and cathode flow rate uncertainties were ≤1% of the set value.

D. Thrust Stand

The thrust levels of the HiVHAc+ Hall thruster were measured with an inverted pendulum null-type thrust stand. The NASA GRC high-power thrust stand has an accuracy of ≤1% based on a statistical analysis of the calibration and thrust zero data taken throughout the test campaign [18]. The operation and theory of the inverted pendulum null-type thrust stand are described in detail in Refs. [19] and [20]. The high-power thrust stand was operated in a

null-type configuration, which allows the thruster to remain stationary while testing. The thrust stand was also equipped with a closed loop inclination control circuit, which utilized a piezoelectric element to minimize thermal drift during thruster operation. The thrust stand was calibrated in-situ with known masses on a pulley system connected to a stepper motor. The thrust stand was calibrated before and after each performance mapping period.

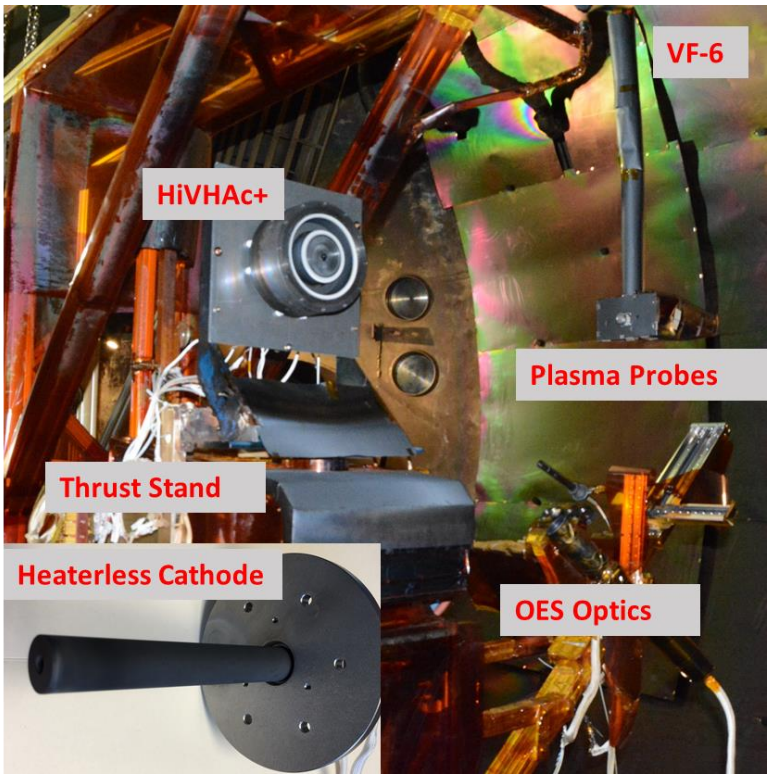

Figure 5. The HiVHAc+ thruster setup inside NASA GRC VF-6 thrust stand. Shown in the left hand corner is the heaterless cathode assembly.

IV. HiVHAc+ Thruster Performance Test Results

In this section the HiVHAc+ thruster flow uniformity and hot-fire performance characterizations test results are reported.

A. Flow Uniformity

The HiVHAc+ flow uniformity was assessed at flow rates of 5, 7.5, 10, 12.5, and 15-mg/s. Table 2 below summarizes test conditions for the flow uniformity test. The 50% axial distance represents the midway distance between the anode downstream face and the thruster's exit plane; whereas, the 100% axial location represents the thruster's exit plane. The 25% and 50% radial locations are the radial locations normalized to the discharge channel half width with the channel centerline being the zero radial location.

Table 2. The HiVHAc+ thruster flow uniformity test conditions. Note that at flow rates of 7.5 and 15-mg/s tests were also performed at elevated facility background pressure (P2× is double base pressure).

Flow Rates, mg/s	Azimuthal Angles,°	Axial Location, %	Radial Location,%
5, 7.5, 10, 12.5, 15	0-360	50%	CL (0%)
5, 7.5, 10, 12.5, 15	0-360	50%, 75%, 100%	CL (0%)
7.5, 15	0-360	50%, 75%, 100%	-50%, -25%, CL (0%), 25%, 50%
7.5 (P2×, P4×, P5×, P6×)	0-360	50%	CL (0%)
15 (P2×)	0-360	50%	CL (0%)

Figure 6 presents the flow uniformity test results at flow rates of 5, 7.5, 10, 12.5, and 15-mg/s along the discharge chamber radial centerline at an axial distance of 50% from the anode face. Results in Fig. 6 show that for all flow rates the flow uniformity is within ±2 %. Profiles presented in Fig. 6 show that the largest flow non-uniformity in the flow rate occurs at the propellant inlet port and 180° opposite to it. The HiVHAc+ flow uniformity of ±2% exceeds the flow uniformity that the Hall thruster community agreed to be acceptable for efficient thruster operation [21, 22]

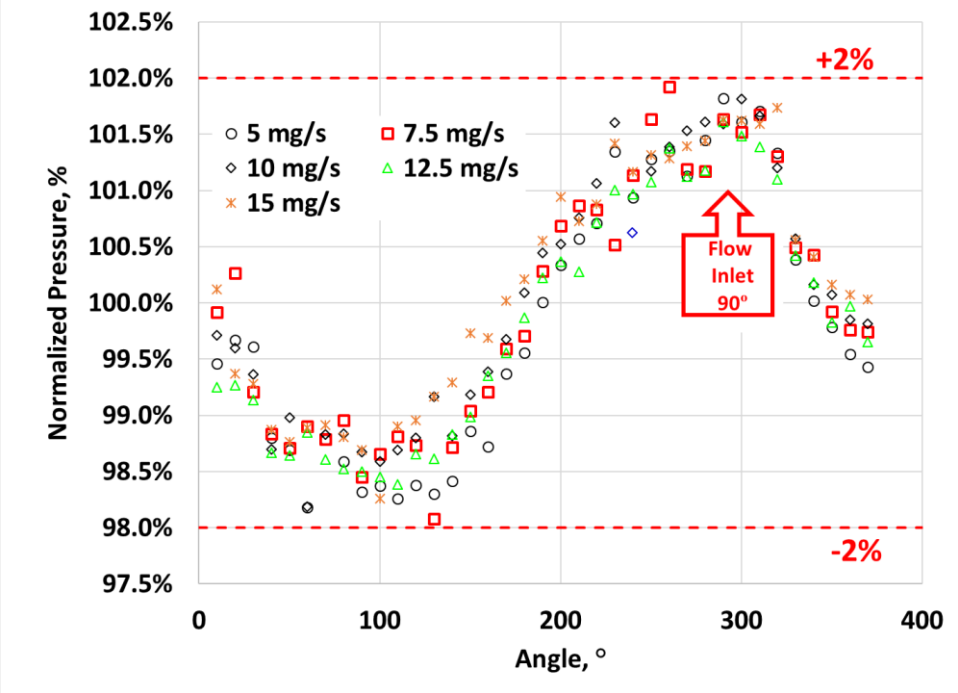

Figure 6. HiVHAc+ thruster flow uniformity profiles along the discharge channel radial centerline at an axial distance of 50% from flow rates of 5, 7.5, 10, 12.5, and 15-mg/s.

B. HiVHAc+ Thruster Performance

The HiVHAc+ thruster performance was assessed at discharge voltages of 300, 400, 500, and 600 V at discharge power levels of 1.5, 3, 4.5, and 6 kW. During the performance assessment, the thruster's normalized peak magnetic field setting was varied between 0.75 and 1.25, with 1.0 referring to the nominal magnetic field setting. Total thrust efficiency (hereafter referred to as thrust efficiency) and total specific impulse (hereafter referred to as specific impulse) results are presented in this section.

Figures 7a and 7b present thrust efficiency and specific impulse magnitudes, respectively, for thruster operation at a discharge voltage of 300-V as a function of the normalized field setting. At 1.5-kW (I_d=5-A) the total thruster efficiency of ~ 48% was mostly invariant to changes in the magnetic field setting and the specific impulse varied between 1,530-sec and 1,620-sec as the thruster's magnetic field was varied over the entire range. Increasing the discharge power to 3-kW (I_d =10-A) increased the thrust efficiency to ~57% and the efficiency was mostly invariant to changes in the magnetic field setting. The specific impulse varied between 1,770-sec and 1,810-sec. At 4.5-kW (I_d=15-A), the thrust efficiency varied between 48% (@ the lowest field setting) and 58% and the specific impulse varied between 1,820-sec and 1,920-sec, with increased magnetic field strength. At 6-kW (I_d=20-A), thrust efficiency varied between 50% and 58% (increasing with increased field strength) and the specific impulse varied between 1,920-sec and 1,990-sec. The results in Fig. 7a indicates that a dramatic increase in performance occurred as the thruster's discharge current was increased from 5-A to 10-A indicating that more efficient performance is achieved as the thruster's operational current density is increased.

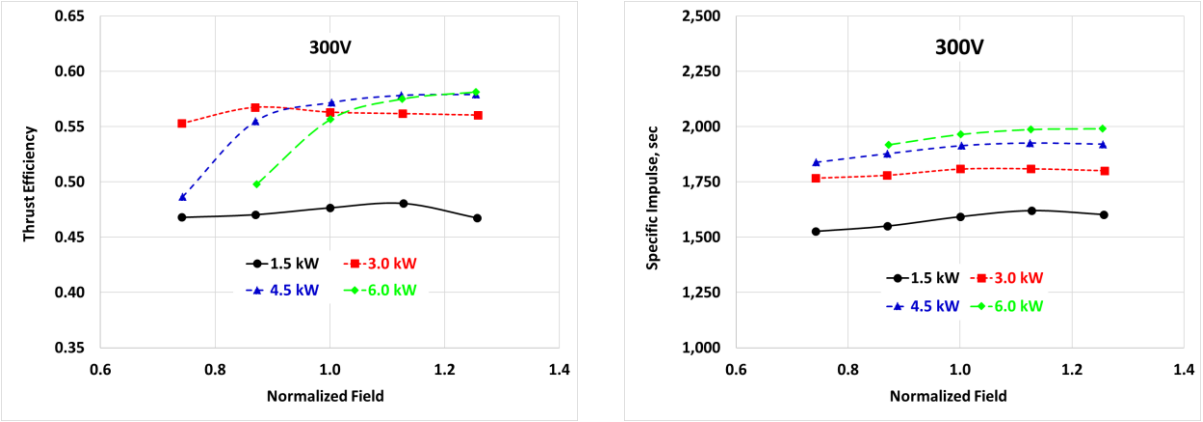

(a) **(b)**

Figure 7. HiVHAc+ thrust efficiency and specific impulse magnitudes as a function of the normalized magnetic field at a discharge voltage of 300-V for discharge power operation of 1.5, 3, 4.5, and 6-kW.

Figures 8a and 8b present thrust efficiency and specific impulse magnitudes, respectively, for thruster operation at a discharge voltage of 400-V as a function of the normalized field setting. At 1.5-kW (I_d=3.75-A) the thrust efficiency varied between 30% and 41% and specific impulse varied between 1,530-sec and 1,720-sec as the normalized magnetic field strength was increased from 0.75 to 1.25. Increasing the discharge power from 1.5-kW to 3-kW (I_d =7.5-A) resulted in a significant increase in thrust efficiency; the thrust efficiency varied between 53% and 56% and specific impulse varied between 1,970-sec and 2,010-sec. At 4.5-kW (I_d=11.25-A), the thrust efficiency varied between 56% and 58% and the specific impulse was almost constant at 2,110-sec as the magnetic field strength was increased. Finally, at 6-kW (I_d=15-A), thrust efficiency varied between 44% (@ lowest field setting) and 60% (increasing with increased field strength) and the specific impulse varied between 2,090-sec and 2,230-sec. Results in Fig. 8a indicate that a dramatic increase in performance occurred as the thruster's discharge current was increased from 3.75-A to 7.5-A indicating that more efficient performance is achieved as the thruster's operational current density is increased (similar to trend at 300-V thruster operation).

Figures 9a and 9b presents thrust efficiency and specific impulse magnitudes, respectively, for thruster operation at a discharge voltage of 500-V as a function of the normalized field setting. At 1.5-kW (I_d=3-A) the thrust efficiency varied between 22% and 38% and specific impulse varied between 1,530-sec and 1,860-sec as the normalized magnetic field strength was increased from 0.75 to 1.25. Increasing the discharge power from 1.5-kW to 3-kW (I_d =6-A) resulted in a significant increase in thrust efficiency; the thrust efficiency varied between 49% and 53% and specific impulse varied between 2,090-sec and 2,180-sec. At 4.5-kW (I_d=9-A), the thrust efficiency varied between 54% and 58% and the specific impulse varied between 2,230-sec and 2,350-sec magnetic field strength was increased. Finally, at 6-kW (I_d=12-A), thrust efficiency varied between 57% and 60% and the specific impulse varied between 2,370-sec and 2,410-sec. Results in Fig. 9a indicate that a dramatic increase in performance occurred as the thruster's discharge current was increased from 3-A to 6-A to 9-A indicating that more efficient performance is achieved as the thruster's operational current density is increased.

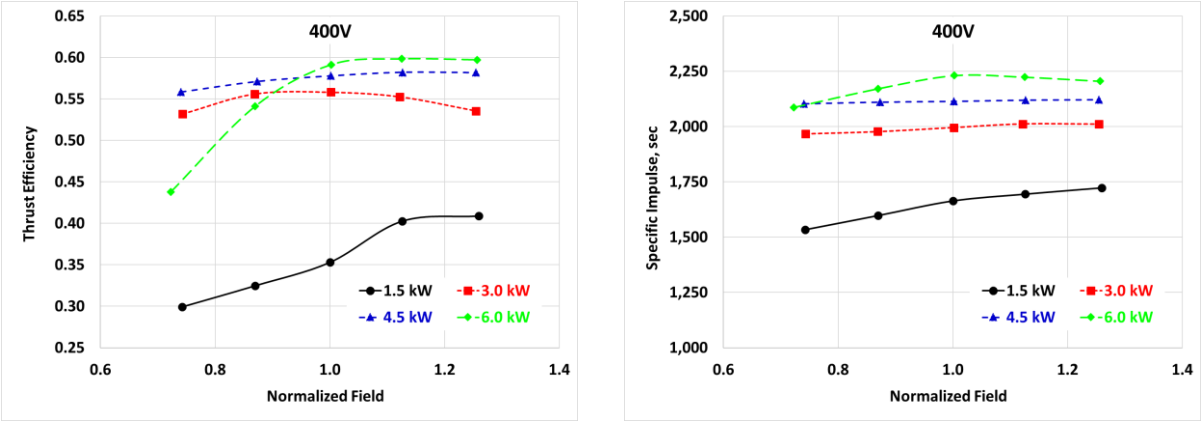

(a) **(b)**

Figure 8. HiVHAc+ thrust efficiency and specific impulse magnitudes as a function of the normalized magnetic field at a discharge voltage of 400-V for discharge power operation of 1.5, 3, 4.5, and 6-kW.

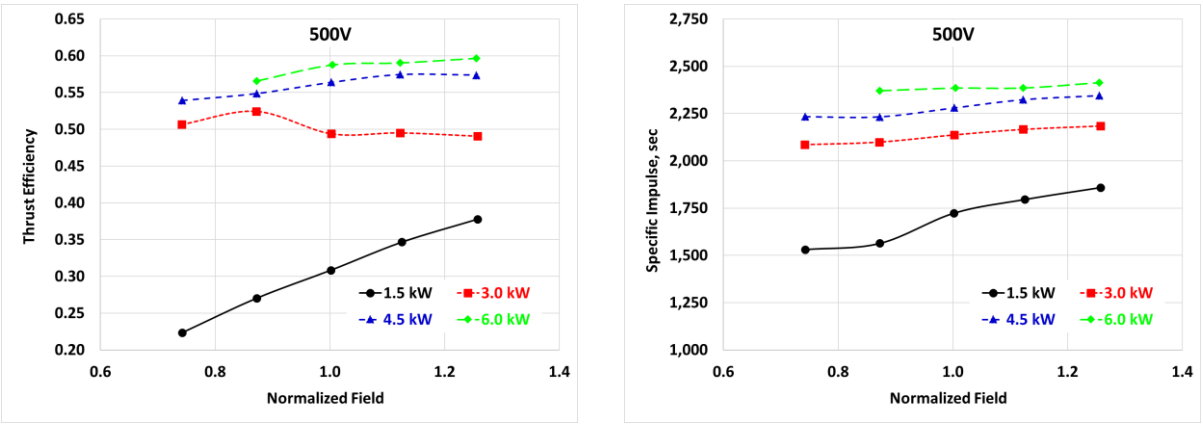

(a) **(b)**

Figure 9. HiVHAc+ thrust efficiency and specific impulse magnitudes as a function of the normalized magnetic field at a discharge voltage of 500-V for discharge power operation of 1.5, 3, 4.5, and 6-kW.

Figures 10a and 10b presents thrust efficiency and specific impulse magnitudes, respectively, for thruster operation at a discharge voltage of 600-V as a function of the normalized field setting. At 1.5-kW (I_d=2.5-A) the thrust efficiency varied between 20% and 34% and specific impulse varied between 1,610-sec and 1,780-sec as the normalized magnetic field strength was increased from 0.75 to 1.25. Increasing the discharge power from 1.5-kW to 3-kW (I_d =5-A) resulted in a significant increase in thrust efficiency; the thrust efficiency varied between 48% and 50% and specific impulse varied between 2,190-sec and 2,370-sec. At 4.5-kW (I_d=7.5-A), the thrust efficiency varied between 53% and 57% and the specific impulse varied between 2,360-sec and 2,550-sec as the magnetic field strength was increased. Finally, at 6-kW (I_d=10-A), thrust efficiency was almost constant at 57% and the specific impulse varied between 2,490-sec and 2,560-sec; thruster operation at the lowest and highest field setting was not attainable due to very high discharge current oscillations. Results in Fig. 10a indicate that a dramatic increase in performance occurred as the thruster's discharge current was increased from 2.5-A to 5-A to 7.5-A indicating that more efficient performance is achieved as the thruster's operational current density is increased.

Figure 11 presents the thrust efficiency as a function of the normalized operating current density (normalized for I_d=7.5-A operation). Profiles in Fig. 11 show that performance improves with increased current density and that close to peak performance for all operating discharge voltages is achieved at a normalized current density of 1.5 . This corresponds to operating the thruster at a discharge current of ~10-A. Additionally, results in Fig. 11 also indicate that slight reductions in the discharge channel area can be made to achieve higher performance at 4.5 kW for all thruster operating voltages. The HiVHAc+ thruster performance is very similar to SOA commercial Hall

thrusters. The thrust efficiencies and specific impulse magnitudes presented in Figures 7, 8, 9, and 10 are in-line with what has been demonstrated by the SPT-140 and BPT-4000 thrusters [23, 24 ,25, 26].

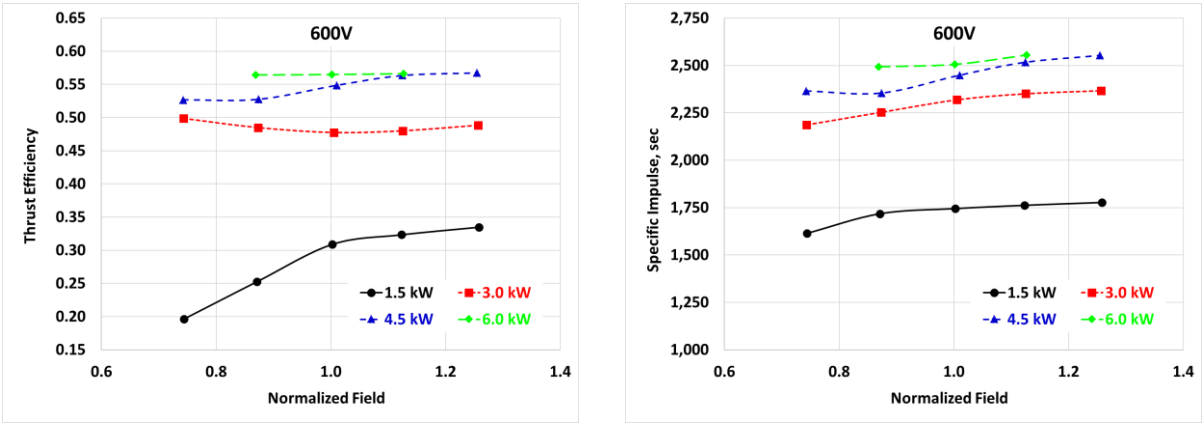

(a) **(b)**

Figure 10. HiVHAc+ thrust efficiency and specific impulse magnitudes as a function of the normalized magnetic field at a discharge voltage of 600-V for discharge power operation of 1.5, 3, 4.5, and 6-kW.

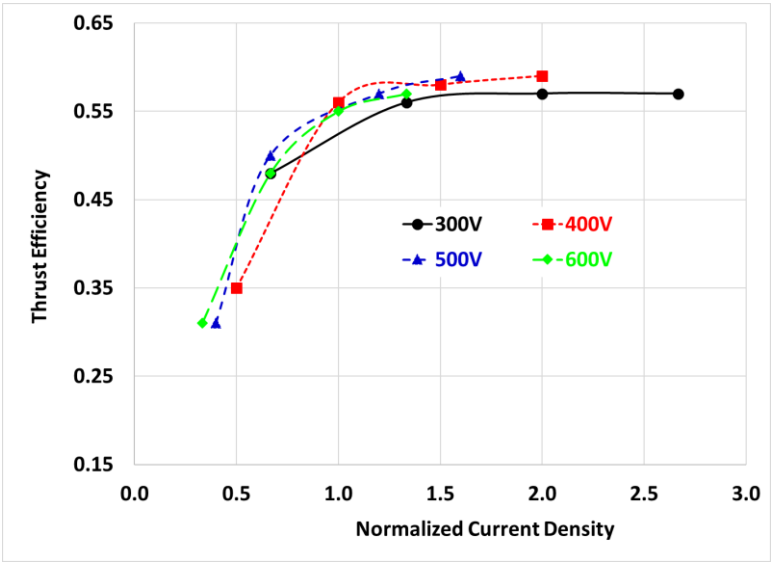

Figure 11. HiVHAc+ thrust efficiency magnitudes as a function of the normalized current density for discharge voltage operation of 300-V, 400-V, 500-V, and 600-VV and at a normalized magnetic field setting of one.

V. HiVHAc System Development Activities

NASA GRC is continuing the HiVHAc system development activities. The upcoming activities are centered around the continued development of the CPE PPU, HiVHAc+ thruster, and the performance of integrated system tests incorporating the VACCO XFCM.

The CPE PPU development will be continued through a NASA Announcement of Collaborative Opportunity (ACO). The ACO selection was announced in July, 2019 and the project will start on October 1, 2019. Through the ACO award, CPE and NASA GRC will further mature the PDU PPU by enhancing its capability and by performing integrated system tests with NASA and commercial Hall thrusters.

The recently awarded ACO project effort will advance the PDU PPU operational readiness by performing functional and integrated system tests of the PDU PPU and VACCO XFCM with up to four different Hall thrusters at NASA GRC. As part of the ACO project and while NASA GRC is awaiting the delivery of the PDU PPU (Spring

2020), integrated system testing of CPE's EM PPU/HiVHAc+/XFCM will be performed to finalize the control algorithms and system parameters (gains, time delays, ramp rates, etc.) required to properly control and operate the entire EP system string. This system-level testing campaign of the EM PPU will also enable critical accumulation of operational hours that are needed to resolve potential latent problems that manifest during long-duration testing. The awarded effort will also implement several additional firmware functionalities for the PPU that will significantly improve system performance, improve reliability, and reduce risk compared to other SOA systems. After delivery of the PDU PPU it will be subjected to a thorough test plan including, functional/performance, vibration, EMI/EMC, and thermal vacuum to qualification levels. The PDU will then be integrated with the HiVHAc+, HERMeS (@ 4.5 kW), and commercial Hall thrusters. After completion of the integrated tests, a long-duration (>500 hours) test will be performed with the HiVHAc+ thruster.

As part of ACO project, CPE will contribute significant additional resources to further the capability of the PDU PPU. This work includes:

- Integration of updated DCIU algorithms in the PDU PPU. NASA GRC will generate the updated algorithm flow charts and will perform checkout tests with the EM PPU. The upgraded algorithms are intended to improve the robustness, flexibility, and operational reliability of the PPU and will then be implemented in the PDU PPU;
- Addition of two nonvolatile multichip memory modules (MCM) to the PDU PPU. The MCMs will be compatible with traditional asynchronous static random-access memory (SRAM) operations and are capable of storing approximately 6 hours of logging data. This new capability will not require any real time communication with flight the computer. The logging will be started upon receiving command from the spacecraft computer;
- Development of PDU PPU firmware to perform thruster current-voltage-magnetic field (IVB) maps of the thruster. This feature that will allow in-flight assessment of the Hall thruster's stability and health. This feature does not exist in SOA PPUs but has been categorized as a critical feature to add to PPU functionality for reasons mentioned above; and
- Development of PDU PPU firmware to implement a xenon flow meter telemetry capability that will enhance in-space performance assessment. This is also a critical feature that will allow the EP system to accurately monitor xenon consumption and to also assess thruster operation in space versus in-ground test facilities.

As for the HiVHAc+ thruster continued development, a new hollow cathode assembly that is based on heritage NASA flight hollow cathode assembly designs is being manufactured. Lessons-learned from the preliminary HiVHAc+ thruster performance characterization test campaign are being incorporated in an updated thruster design to improve its performance. Additionally, as part of the EM PPU/HiVHAc thruster initial test campaign, assessment of the thruster's stability will also be performed.

VI. Summary and Future Work

The development of the HiVHAc Hall propulsion system is on-going. The primary components of the HiVHAc propulsion system include the HiVHAc+ thruster, the CPE PDU PPU, and the VACCO XFC unit.

The NASA funded CPE PDU PPU development is ongoing. The PDU PPU will be delivered to NASA GRC in the Spring of 2020. The PDU includes complete form, fit and function for flight and all electrical, electronic and electromechanical parts that are rad-hard, space-qualified or have exact equivalents. The PDU has higher discharge power capability up to 4.5-kW. The PDU also has a modified input voltage range of 68-V to 140-V to better satisfy commercial spacecraft bus voltages and still satisfy typical NASA deep space mission power requirements. Output requirements for the thruster electromagnet and heater power supplies were also extended to capture the requirements of multiple thrusters including NASA's HiVHAc+ as well as commercial Hall thrusters.

NASA GRC HiVHAc+ thruster development is also ongoing. NASA STMD CIF funding resulted in the design, manufacture, and test of 4.5 kW-class throttleable Hall thruster with a centrally mounted cathode that has demonstrated thrust efficiencies of 58% at 4.5 kW. Further refinements to the thruster design, incorporating lessons-learned from the HiVHAc+ thruster initial test campaign are being performed.

As for the VACCO XFCM unit, NASA GRC will leverage the XFC unit that is being developed under the AEPS project. The AEPS project VACCO XFC unit is based on the XFCM unit with slight modifications to improve performance and flow accuracy.

Finally, CPE was recently awarded a NASA ACO project to further the development of the PDU PPU. Under the ACO project the PDU PPU will incorporate additional capabilities and integrated testing at NASA GRC will be performed with NASA and commercial Hall thrusters.

Acknowledgments

The authors would like to thank and acknowledge the Science Mission Directorate, NASA Space Technology mission Directorate, NASA SBIR program, and NASA GRC for supporting the CPE PPU and HiVHAc+ development. The authors would like to thank Michael McVetta, Luke Sorrelle, Kevin Blake, David Yendriga, and Derrick Patterson, for supporting the assembly and installation of the thruster in the vacuum facility, as well as maintaining and operating the vacuum facility.

References

[1] Dankanich, J. W., "Electric Propulsion for Small Body Missions", AIAA Paper 2010-6614, August 2010.
[2] Brophy, J., Garner, C., Nakazono, B., Marcucci, M., Henry, M., and Noon, D., "The ion Propulsion System for Dawn," AIAA-2003-4542, July, 2003.
[3] Garner, C.E., Rayman, M.D., and Brophy, J.R., "In-Flight Operation of the Dawn Ion Propulsion System Through Year One of the Cruise to Ceres," AIAA-2013-4112, July 2013.
[4] Dankanich, J.W., Drexler, J. A., and Oleson, S. R., "Electric Propulsion Mission Viability with the Discovery-Class Cost Cap," AIAA Paper 2010-6776, August 2010.
[5] Kamhawi, H., Haag, T., Pinero L., Huang, W., Peterson., T, Manzella, D., Dankanich, J., Mathers, A., and Hobson, D., "Overview of the Development of a Low Cost High Voltage Hall Accelerator Propulsion System for NASA Science Missions," AIAA-2011-5520, presented in the 47th AIAA/ASME/SAE/SEE Joint Propulsion Conference, July 2011, San Diego, CA.
[6] Pinero, L. R., Kamhawi, H., and Drummond, G., "Integration Testing of a Modular Discharge Supply for NASA's High Voltage Hall Accelerator Thruster," IEPC Paper 2009-275, September 2009.
[7] Pinero, L.R, Kamhawi, H., and Shilo, V., "Performance of a High-Fidelity 4 kW-Class Engineering Model PPU and Integration with HiVHAc System," AIAA-2016-5031, presented in the 52nd AIAA/SAE/ASEE Joint Propulsion Conference, Salt Lake City, Utah, July 2016.
[8] J. M. Cardin, W. Cook, and R. Bhandari, "Qualification of an Advanced Xenon Flow Control Module," in *33rd International Electric Propulsion Conference*, Washington, DC, 2013.
[9] Dankanich, J., Cardin, J., Dien, A., Kamhawi, H., Netwall, C., and Osborn, M., "Advanced Xenon Feed System (AXFS) Development and Hot-fire Testing," 45th AIAA Joint Propulsion Conference, AIAA 2009-4910, Denver, Colorado, USA, August 2-5, 2009.
[10] Kamhawi, H., Haag, T., Huang, W., Shastry, R., Pinero, L., Peterson, T., and Mathers, A., "Performance and Environmental Test Results of the High Voltage Hall Accelerator Engineering Development Unit," AIAA-2012-3854, presented in the 48th AIAA/ASME/SAE/ASEE Joint Propulsion Conference, Atlanta, GA, July 2012.
[11] Kamhawi, H., Huang, W., Haag, T., and Spektor, R., "Investigation of the Effects of Background Pressure on the Performance and Voltage-Current Characteristics of the High Voltage Accelerator," AIAA-2014-3707, presented in the 50th AIAA/ASME/SAE/ASEE Joint Propulsion Conference, Cleveland, OH, July 2014.
[12] Hofer, R., Johnson, L., Goebel, D., and Fitzgerald, D., "Effects of an Internally Mounted Cathode on Hall Thruster Plume Properties," AIAA-2006-4482, presented in the 42nd AIAA/ASME/SAE/ASEE Joint Propulsion Conference, Sacramento, CA, July 2006.
[13] Huang., W, and Yim, J., " Propellant Distributor for a Thruster," April, 2019, US Patent 10273944.
[14] Farnell, C, Farnell, C., Williams, J., Williams, D., Nguyen, B., Greiner, K., and Ham, R., "Simplified Formation Process of a Low Work Function Insert," June 2018, US Patent 10002738.
[15] Kamhawi, H., Pinero, L., Haag, T., Huang, W., Ahern, D., Liang, R., and Shilo, V., "Integration Tests of the 4 kW-class High Voltage Accerlator Power Processing Unit with the HiVHAc and the SPT-140 Hall Effect Thrusters," AIAA-2016-4943, presented in the 52nd AIAA/ASME/SAE/ASEE Joint Propulsion Conference, Salt Lake City, UT, July 2016.
[16] Patterson, M. J., and Sovey, J. S. "History of Electric Propulsion at NASA Glenn Research Center: 1956 to Present," *Journal of Aerospace Engineering* Vol. 26, No. 2, 2013, pp. 300-316.

[17] P. Y. Peterson, H. Kamhawi, W. Huang, J. Yim, T. W. Haag, J. Mackey, M. McVetta, L. Sorrelle, T. Tomsik, R. Gilligan, and D. Herman, "Reconfiguration of NASA GRC's Vacuum Facility 6 for Testing of Advanced Electric Propulsion System (AEPS) Hardware," presented at the 35th International Electric Propulsion Conference, IEPC-2017-028, Atlanta, GA, 2017.
[18] Mackey, J. A., Haag, T. W., Kamhawi, H., Hall, S. J., and Peterson, P. Y., "Uncertainty in Inverted Pendulum Thrust Measurements," NASA/TM-2018-219952.
[19] T. W. Haag, "Thrust stand for high-power electric propulsion devices," *Review of Scientific Instruments,* vol. 62, 1991 1991.
[20] T. W. Haag and M. Osborn, "RHETT/EPDM performance characterization," in *International Electric Propulsion Conference, IEPC-97-107,* Cleveland, OH, 1997.
[21] Reid, B. M., "The Influence of Neutral Flow Rate in the Operation of Hall Thrusters," Ph.D. dissertation, University of Michigan, 2009.
[22] Huang, W., and Yim, J., "Propellant Distributor for a Thruster". USA Patent 10,273,944, 30 April 2019.
[23] De Grys, K., Rayburn, C., Wilson, F., Fisher, J., Werthman, L., and Khayms, V., "Multi-Mode 4.5 kW BPT-4000 Hall Thruster Qualification Status," AIAA-2003-4552, presented in the 39th AIAA/ASME/SAE/ASEE Joint Propulsion Conference Huntsville, AL, July 2003.
[24] Hofer, R., "High Specific Impulse Operation of the BPT-4000 Hall Thruster for NASA Science Missions," AIAA_2010-6623, presented in the 46th AIAA/ASME/SAE/ASEE Joint Propulsion Conference Nashville, TN, July 2010.
[25] Glogowski, M., Kodys, A., Pilchuk, J., Hartmann, J., Lentati, A., Kadakkal, V., Pulido, C, Trescott, J., Pucci, J., and Koch, B., "Design, Qualification, and Initial Flight Operations of The GeoStar-3 Electric Propulsion System," AIAA-2018-4719, presented in the 54th AIAA/ASME/SAE/ASEE Joint Propulsion Conference Nashville, TN, July 2010.
[26] Snyder, S., Lenguito, G., Frieman, J., Haag, T., and Mackey, J., "The Effects of Background Pressure on the SPT-140 Hall Thruster Performance," AIAA-2018-4421.